

Fabrication of colloidal self-assembled monolayer (SAM) using monodisperse silica and its use as a lithographic mask

Hwa-young Ko^a, Hae-Weon Lee^b, Jooho Moon^{a,*}

^aDepartment of Ceramic Engineering, Yonsei University, Seoul 120-749, South Korea

^bNano-Materials Research Center, KIST, Seoul 136-791, South Korea

Abstract

Monodisperse colloidal silica with controlled sizes (100, 200 and 300 nm) has been prepared by the Stöber process. The shape and monodispersity of the synthesized colloidal particles were observed by scanning electron microscopy and laser light scattering particle analyzer. Self-assembled monolayer (SAM) of monodisperse colloids was obtained by dipping a Si substrate into a well-dispersed silica suspension. It was found that the uniformity and spatial extent of colloidal SAM were significantly influenced by the experimental parameters such as concentration, pH and surface tension of the colloidal suspension. We have observed a hexagonally well-ordered packing colloidal monolayer in a relatively large area ($1.5 \times 1.5 \text{ mm}^2$). The platinum was sputtered over the colloidal SAM used as a lithographic mask. This produced a honeycomb-shaped patterned Pt structure of thickness $\sim 60 \text{ nm}$ on the Si substrate after the removal of the colloidal silica.

© 2003 Elsevier B.V. All rights reserved.

Keywords: Monodisperse colloidal silica; Self-assembled monolayer; Patterned Pt structure

1. Introduction

Investigation of the self-assembling of materials has become one of the most popular research topics in recent years. There are several objects that exhibit possible self-assembling characteristics such as surfactant, block copolymer and colloidal particles in an increasing order of the object sizes. Each self-assembling object has received significant research interest for a wide variety of applications ranging from detergent to microelectronics [1]. Among these, colloidal particles, defined as small materials with at least one characteristic dimension in the range of $1 \text{ nm} - 1 \mu\text{m}$, have long been used as major components of various industrial products such as inks, paints, catalysts, coatings, papers, cosmetics and photographic films [2,3]. In particular, spherical monodisperse colloidal particles may represent the simplest form of building blocks that can readily be self-assembled into 2D and 3D ordered lattices on a planar substrate such as colloidal crystals or synthetic opals

[4–8]. The ability to crystallize spherical colloids into spatially periodic structures has allowed us to obtain interesting and often useful functionality not only from the colloidal materials, but also from the long-range order exhibited by these crystalline lattices. The colloidal crystals can find themselves useful in a wide variety of applications such as optical filters/switches [9], catalyst [10], photonic crystal [11], chemical/biological sensor [12] and lithographic mask [13].

The fabrication routes for creating colloidal crystals can be roughly divided into two techniques: gravity sedimentation [14] and solvent evaporation [15]. In the gravity sedimentation method, crystal formation can only occur at specific colloid volume fractions. As a result, the crystal thickness is not easily controlled. For the solvent evaporation method, a 2D colloid crystal can be obtained, and the thickness can be controlled by either varying colloid concentrations or repeated layer-by-layer crystallization [16,17]. Dip coating is the most popular method in which the colloids are evaporation-induced and self-assembled on the substrate as it is slowly withdrawn from the colloid suspension.

The present paper focuses on the 2D self-assembly of monodisperse colloids and studies their self-assembly mechanisms taking place during dip coating. We have

*Corresponding author. Tel.: +82-2-2123-2855; fax: +82-2-365-5882.

E-mail address: jmoon@yonsei.ac.kr (J. Moon).

Table 1

Various synthesis composition for colloidal silica and its particle size distribution

Sample No.	Concentration of constituents (mole)				Particle size distribution (nm)			
	TEOS	NH ₃	H ₂ O	Ethanol	D ₁₀	D ₅₀	D ₉₀	σ
1	0.10	1.10	8.80	13.59	134.1	151.3	167.7	27.1
2	0.40	1.20	6.40	13.15	198.7	221.7	241.9	32.7
3	0.40	0.56	7.04	13.21	273.8	284.4	293.6	21.2

synthesized monodisperse colloidal silica with different sizes (100, 200 and 300 nm) by the Stöber process. Self-assembled monolayer (SAM) in a relatively large area was achieved by controlling the experimental parameters such as concentration, pH and surface tension of the colloidal suspension. In addition, we have demonstrated the feasibility for using the colloidal SAM as a lithographic mask to fabricate nano-patterned structures.

2. Experimental

2.1. Preparation of colloidal silica

Monodisperse colloidal silica was synthesized by the Stöber process using TEOS (99.9%, Aldrich Chemical Co.), ethanol (99.9%, Aldrich Chemical Co.), NH₄OH (28% NH₃ in water, Aldrich Chemical Co.) and deionized water as starting materials. The detailed compositions of the reactants are summarized in Table 1. The schematic diagram for preparation of monodisperse colloidal silica is illustrated in Fig. 1. The reactant solution was stirred in water bath (Fisher isotemp heating cir-

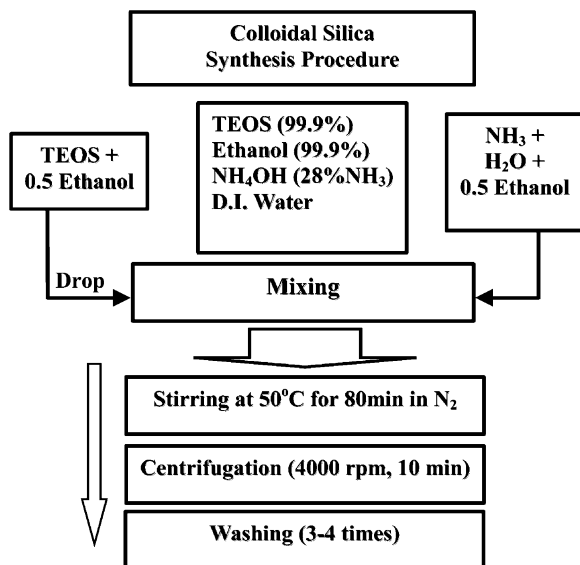


Fig. 1. Synthesis procedure of monodisperse colloidal silica.

culators model No. 2013P) at 50 °C, under N₂ atmosphere. After stirring for 80 min, the sol was repeatedly washed by centrifugation and decantation with ethanol to remove undesirable particles and to prevent continuous reaction followed by drying in a vacuum oven at 100 °C. Morphology and particle size of the synthesized colloidal silica were examined using scanning electron

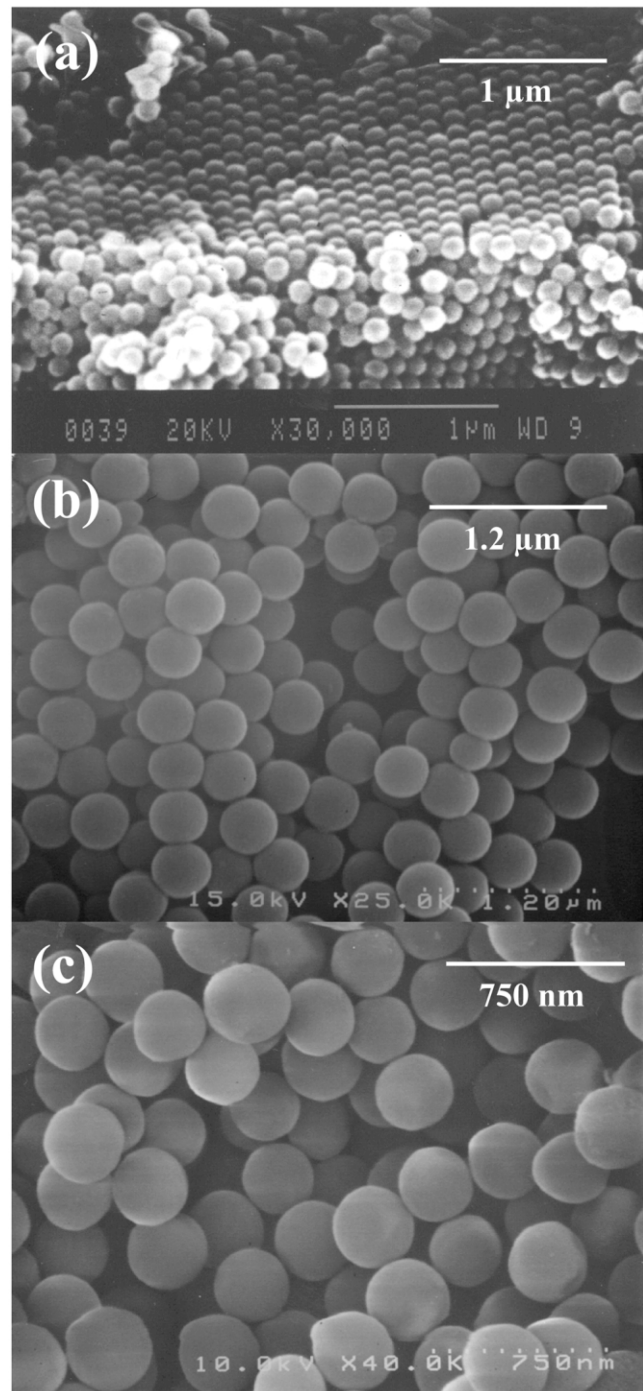


Fig. 2. SEM images of the synthesized colloidal silica: (a) sample 1; (b) sample 2; (c) sample 3.

microscopy (SEM, JEOL JSM6330F) and laser light scattering particle analyzer (Microtrac UPA-150), respectively.

2.2. Preparation of colloidal self-assembled monolayer

A SAM of the monodispersed colloids was achieved by dipping the Si substrate into a well-dispersed suspen-

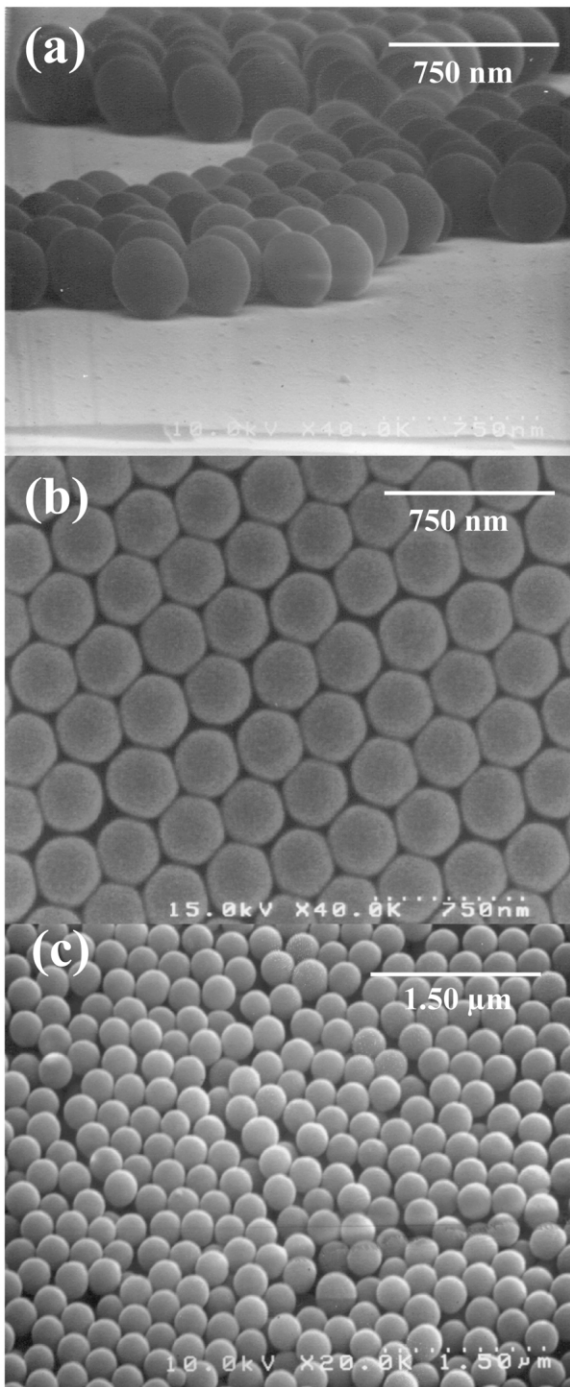


Fig. 3. SEM images of the self-assembled silica on the Si substrate prepared from different solid loading conditions: (a) 0.5 wt.%; (b) 2 wt.%; (c) 5 wt.%.

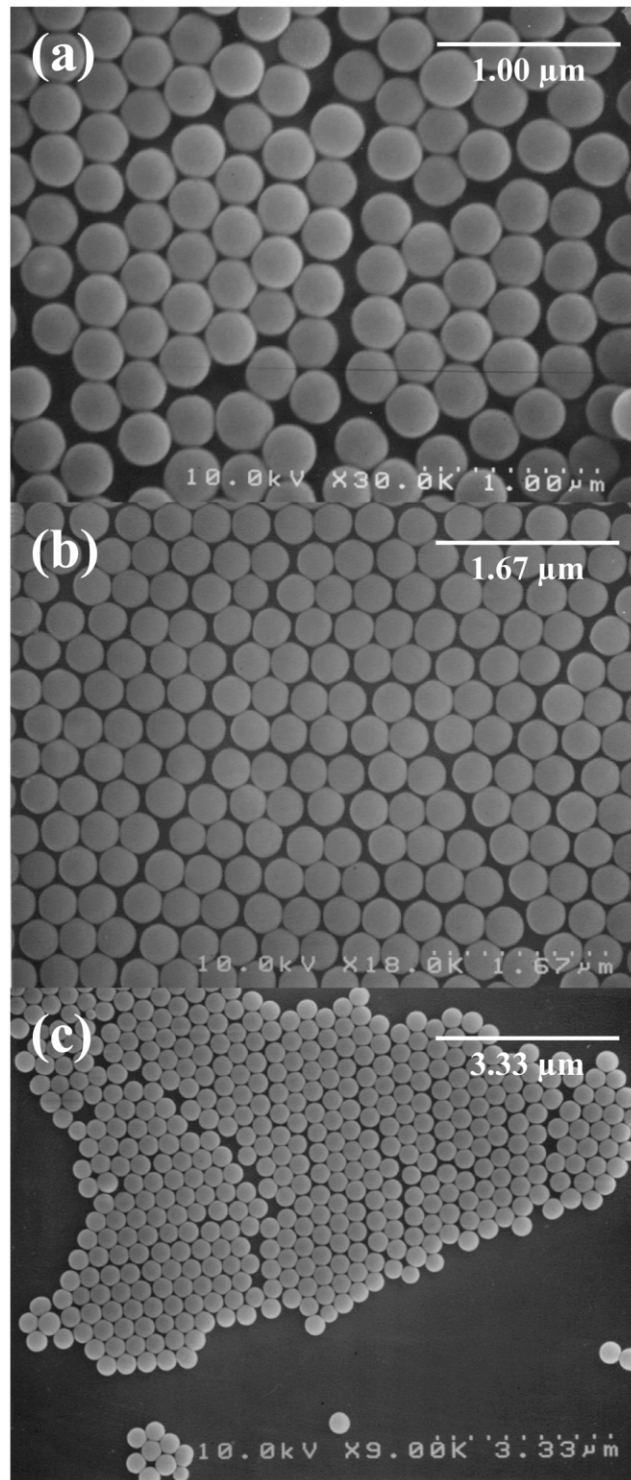


Fig. 4. SEM images of the self-assembled silica on the Si substrate prepared from different solvent systems: (a) water:ethanol=1:4; (b) water:ethanol=1:1; (c) water:ethanol=4:1.

sion with colloidal silica (sample 3: 280.1 ± 21.2 nm). Dip coating was performed by varying experimental parameters such as solid loading (0.5, 2 and 5 wt.%), pH (11.24, 7.12 and 5.56), type of the solvents (etha-

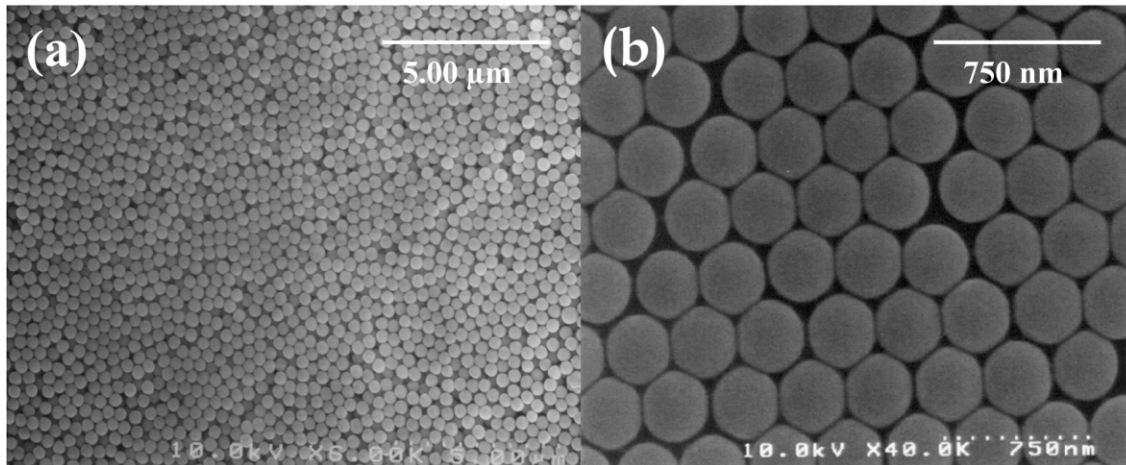


Fig. 5. SEM images of the self-assembled silica on the Si substrate prepared from different pH of the suspension: (a) pH 5.56, pH 7.12; (b) pH 11.24.

nol:water=1:4, 1:1 and 4:1) of the colloidal suspension. Withdrawal speed was fixed to 0.4 cm/min throughout the experiments.

2.3. Fabrication of nano-patterned structures using colloidal SAM

The self-assembled colloids were used as a lithographic mask to produce a nanoscale-patterned structure on the substrate. Platinum was sputtered over the Si substrate on which the self-assembled colloidal monolayer had been formed by dip coating. Sputtering time was 5 min, during which, approximately 60-nm thick Pt layer was deposited. The sample was ultrasonically washed in water for 60 s to remove colloidal silica attached to the Si substrate. Patterned structures were observed by SEM.

3. Results and discussion

SEM pictures of the synthesized colloidal silica are shown in Fig. 2. The colloidal silica has a nearly

monodisperse spherical shape with the particle sizes ranging from 140 to 290 nm depending upon the synthesis conditions. The results of particle size distribution analyses measured by the laser light scattering technique are summarized in Table 1. The mean particle size and its standard deviation for sample 1, sample 2 and sample 3 were 148.7 ± 27.1 , 213.3 ± 32.7 and 280.1 ± 21.2 nm, respectively. The size of the synthesized colloidal silica depends strongly upon the ratio of TEOS and water [18]. With increasing the ratio (sample 1 (TEOS/H₂O=0.0114) → sample 2 (TEOS/H₂O=0.0625)), the size of colloidal silica became larger. Ammonia also apparently influenced the monodispersity of the synthesized particles. An increase in the ratio of ammonia and water (sample 2 (NH₃/H₂O=0.1875) → sample 3 (NH₃/H₂O=0.080)) caused the production of larger particles with improved monodispersity.

The microstructures of the self-assembled silica were prepared at different solid loading conditions as shown in Fig. 3. The solid loading in the colloidal silica suspension varied from 0.5 to 5 wt.%, while all the

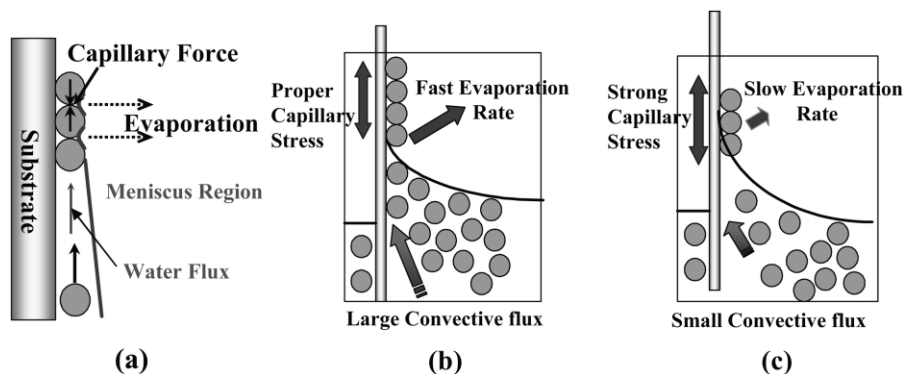


Fig. 6. (a) Colloidal crystallization mechanism during dip coating; (b) a case of large convective flux; (c) a case of small convective flux.

other parameters were kept constant, such as withdrawal speed, pH and type of the solvent. It was observed that self-assembled structures and their spatial extent of colloidal silica on the Si substrate were significantly influenced. When the particle concentration was low (0.5 wt.%), the silica particles adhered to a limited region of the substrate, forming scattered small islands composed of close-packed silica particles (Fig. 3a). On the other hand, at a concentration of 5 wt.%, the silica was self-assembled into a bilayer structure with a reduced packing regularity covering over the large area of the substrate as shown in Fig. 3c. When prepared from the colloidal suspension of 2 wt.%, however, the SAM of silica particles was arranged in a hexagonally well-ordered packing structure in an area of $100 \times 100 \mu\text{m}^2$ as shown in Fig. 3b.

The influence of the solvent types in the colloidal silica suspension was investigated as shown in Fig. 4. Withdrawal speed, solid loading and pH of the suspension were 0.4 cm/min, 2 wt.% and pH 11.24, respectively. When the solvent was a mixture of water and ethanol in a volume ratio of 1:4, a disordered packing of colloidal particles was observed (Fig. 4a), while the assembled colloidal silica was grouped into several islands at the condition of water:ethanol=4:1 (Fig. 4c). In contrast, colloidal monolayer with a better packing structure in a relatively large area was achieved with a ratio of water:ethanol of 1:1 (Fig. 4b). Fig. 5 presents the microstructures of the self-assembled colloidal silica prepared at different pH of the suspension ranging from pH 5.56 to pH 11.24 at the conditions of 2 wt.% solid loading, 0.4 cm/min withdrawal speed, and ratio of water and ethanol=1:1. At the conditions of both pH 5.56 and 7.12, silica particles were accumulated in multilayers in the large area as shown in Fig. 5a. However, at pH 11.24, the SAM of silica particles was arranged in a hexagonally well-ordered packing structure as shown in Fig. 5b.

Self-assembly mechanisms taking place during dip coating are quite complex. Colloidal crystallization occurs at the meniscus region between liquid and gas interfaces formed by withdrawing the substrate. Colloidal particles move towards the upper region of the substrate through a convective flux that is generated by the evaporation of solvent in the meniscus region that is schematically depicted in Fig. 6a. At a proper withdrawal speed, the upper region of the meniscus retreats below the height of the particle monolayer as the solvent evaporates, exposing the particle surface–gas interfaces. At this moment, monodisperse colloids experience attractive capillary force, which allows the colloids packed into an ordered structure, forming a self-assembled colloidal monolayer. The important variables associated with colloidal crystallization by dip coating include the concentration of particle, the evaporation rate and surface tension of the solvent, the surface

charges of the particle and substrate and withdrawal speed, etc. [19]. The concentration of silica suspension determines upward flux of the particles at a given convective flux of liquid. When the particle concentra-

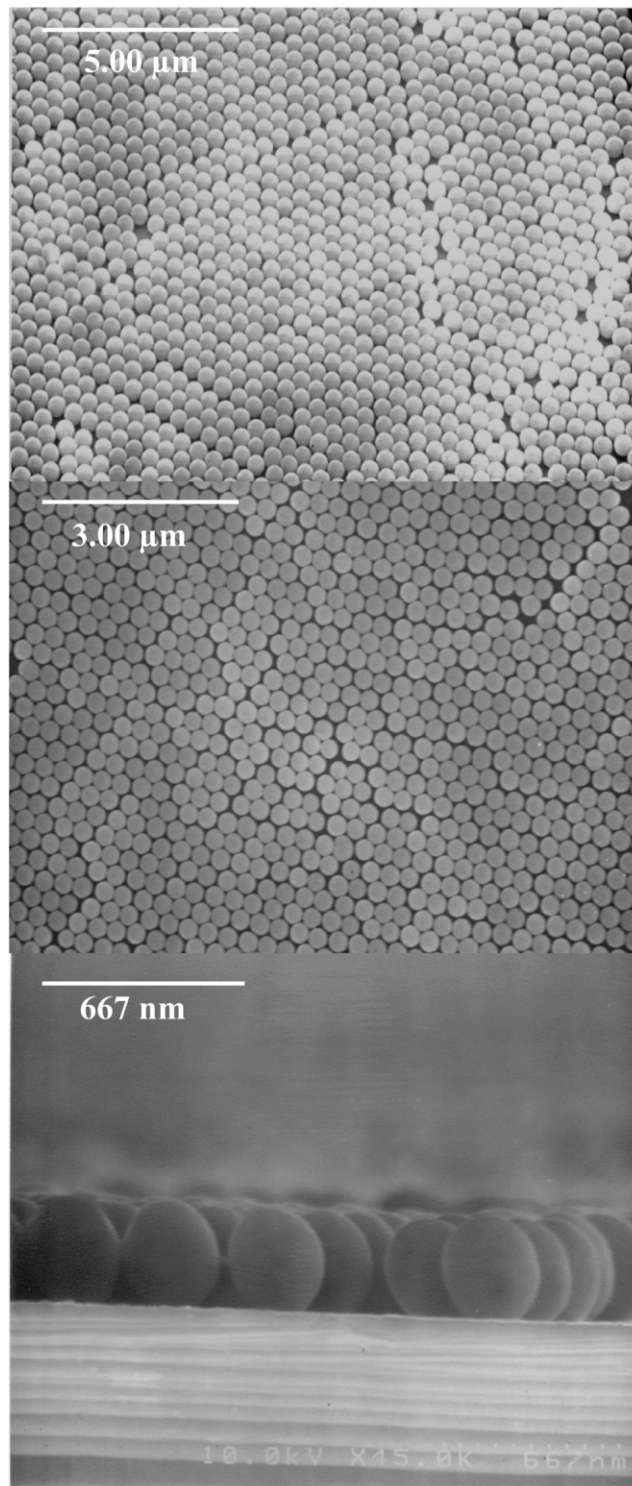


Fig. 7. SEM images of the self-assembled monodispersed silica in a large area.

tion is higher, the particles are accumulated in a multi-layer, covering the large area of the substrate. On the other hand, when the particle concentration is lower, sufficient particles are not supplied to form a uniform monolayer, resulting in scattered islands of SAM as shown in Fig. 3.

The types of the solvent also control both the surface tension and the rate of evaporation. For a solvent with high surface tension, as in the case of water:ethanol=4:1, the meniscus angle is steep so that a thick meniscus is generated as explained in Fig. 6b. In this situation, no sufficient convective flux exists to force the particles transported since the solvent has a relatively low evaporation rate. At the same time, the meniscus can still be maintained as the substrate is raised. The suspension near the meniscus breaks into droplets due to its gravity, falling back to a reservoir. However, for a solvent with low surface tension, as in the case of water:ethanol=1:4, the slope of the meniscus is low and the solvent easily evaporates as shown in Fig. 6c. Although the particles are supplied well towards the upper meniscus region, the capillary forces exerted between the particles are insufficient for forming SAM in a large area because of lower surface tension.

The pH of the colloidal suspension governs the surface charges developed at the surfaces of both the particle and substrate. Franks reported that the surface charge of colloidal silica is negatively charged and the isoelectric point is approximately pH 2 [20]. The silicon

wafer also exhibits negative charge in aqueous solution above pH 2 because of the presence of a thin oxidized layer. The lower the pH of solution, the smaller the magnitude of the negative charge on the colloidal silica and silicon wafer. Hence, a repulsive force between colloidal silica and Si substrate decreases. This enhances adhesion of the particles on the substrate during dip coating, producing a disordered particle arrangement in multi-layers as seen Fig. 5a. When the colloidal suspension of higher pH is used, strong repulsive force between particles is balanced by attractive capillary force, which results in a monolayer of the well-ordered colloidal crystal.

Fig. 7 shows the microstructure of a hexagonally ordered packing colloidal monolayer in a relatively large area of $1.5 \times 1.5 \text{ mm}^2$ under optimized conditions at 0.4 cm/min withdrawal speed, pH 11.24, the ratio of water and ethanol=1:1, and 2 wt.% solid loading. Feasibility testing also indicated that such a monolayer of SAM fabricated in the current study could be used as a lithographic mask. As shown in Fig. 8, 60-nm thick-Pt nano-patterned structure of honeycomb-shape was easily fabricated by sputtering Pt over the colloidal SAM-deposited substrate.

4. Conclusions

We have fabricated a SAM of monodisperse colloidal silica with the mean diameter of $280.1 \pm 21.2 \text{ nm}$ syn-

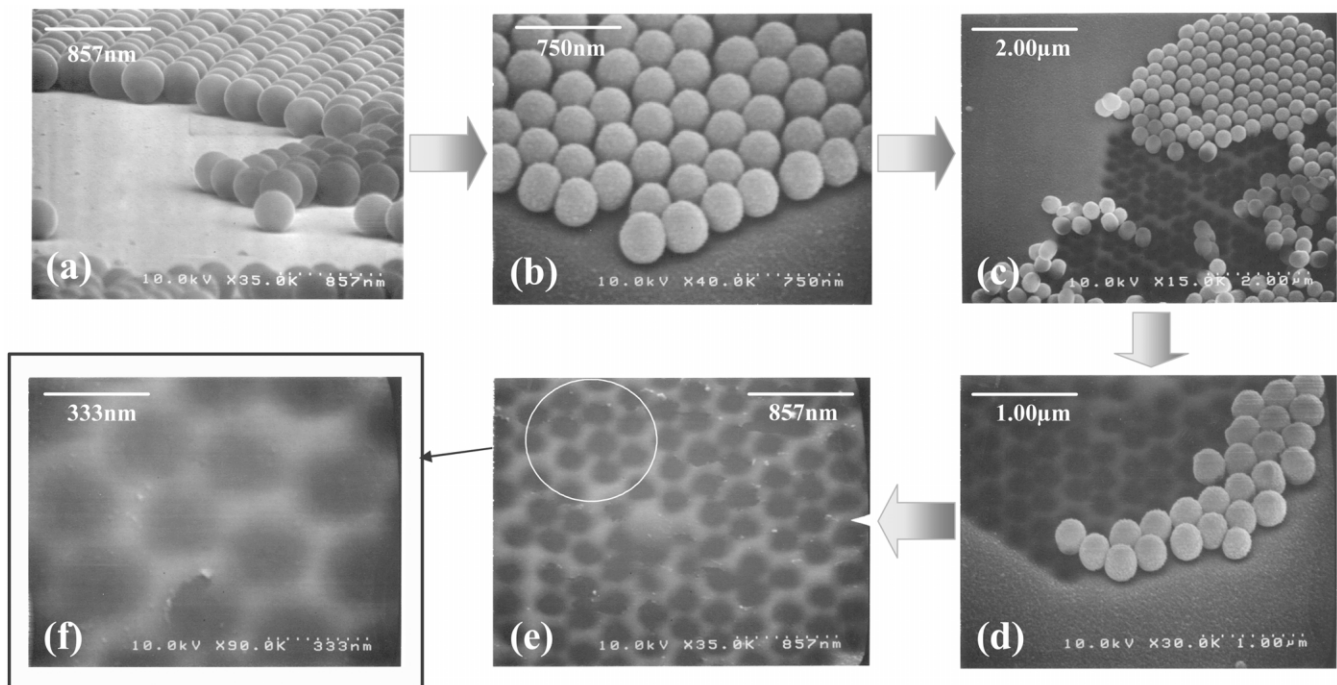


Fig. 8. SEM images of Pt nano-patterned structures: (a) colloid SAM lithographic mask; (b) after sputtering Pt over the colloidal SAM; (c–f) honeycomb-shaped nano-patterned structure after the removal of colloidal silica.

thesized by the Stöber process. Well-dispersed silica particles in a suspension were transferred onto a Si substrate by dip coating, forming a well-ordered hexagonally packed structure in a relatively large area of $1.5 \times 1.5 \text{ mm}^2$. The microstructure and its spatial extent of the SAM were determined by the crystallization mechanisms of the colloids, which were significantly influenced by the solid loading, surface tension, rate of evaporation and pH of the colloidal silica suspension. It was also demonstrated that the colloidal SAM could be used as a lithographic mask. Sputtering over the colloidal SAM produces honeycomb-shaped nano-patterned structure of Pt after removal of the silica particles from the surface of the substrate.

Acknowledgments

This work was supported by a Grant No. R01-2002-000-00318-0 from Korea Science and Engineering Foundation.

References

- [1] J. Zhang, Z.-l. Wang, J. Liu, S. Chen, G.-yu. Liu, *Self-assembled Nanostructures*, Kluwer Academic/Plenum Publishers, New York, 2002, pp. 77–112.
- [2] T. Sugimoto, *Monodispersed Particles*, first ed., Elsevier, Amsterdam, 2001, pp. 59–113.
- [3] H. Geische, K. Osseo-Assare, in: T. Sugimoto (Ed.), *Fine Particles: Synthesis, Characterization, and Mechanisms of Growth*, Surfactant Science, 92, Marcel Dekker, New York, 2000, pp. 126–188.
- [4] Y. Yin, Y. Lu, B. Gates, Y. Xia, *J. Am. Chem. Soc.* 123 (2001) 8718.
- [5] Q.-B. Meng, Z.-Z. Gu, O. Sato, *Appl. Phys. Lett.* 77 (2000) 4313.
- [6] Y. Masuda, M. Itoh, T. Yonezawa, K. Koumoto, *Langmuir* 18 (2002) 4155.
- [7] Y.-H. Ye, S. Badilescu, V.-V. Truong, *Appl. Phys. Lett.* 81 (2002) 616.
- [8] C. Ternon, F. Fourbilleau, X. Portier, P. Voivenel, C. Dufour, *Thin Solid Films* 419 (2002) 5.
- [9] J.C. Night, J. Brogeng, T.A. Birks, P.S.J. Russel, *Science* 282 (1998) 1476.
- [10] K.R. Gopidas, M. Bohorquex, P.V. Kamat, *J. Phys. Chem.* 94 (1990) 6435.
- [11] A. Van Blaaderen, R. Ruel, P. Wiltzius, *Nature* 385 (1997) 321.
- [12] J.H. Holtz, S.A. Asher, *Nature* 389 (1997) 829.
- [13] C.L. Hatnes, A.D. McFarland, M.T. Smith, J.C. Hulteen, R.P. Van Duyne, *J. Phys. Chem. B* 106 (2002) 1898.
- [14] H. Miguez, F. Meseguer, C. Lopez, A. Blanco, J.S. Moya, J. Requena, A. Mifsud, V. Fornes, *Adv. Mater.* 10 (1998) 480.
- [15] N.D. Denkov, O.D. Velev, P.A. Kralchevsky, I.B. Ivanov, H. Yoshimura, K. Nagayama, *Nature* 361 (1993) 26.
- [16] S.M. Yang, H. Miguez, G.A. Ozin, *Adv. Funct. Mater.* 12 (2002) 425.
- [17] P. Jiang, J.F. Bertone, K.S. Hwang, V.L. Colvin, *Chem. Mater.* 11 (1999) 2132.
- [18] W. Stöber, A. Flink, *J. Colloid. Interf. Sci.* 26 (1968) 62.
- [19] N.D. Denkov, O.D. Velev, P.A. Kralchevsky, I.B. Ivanov, H. Yoshimura, K. Nagayama, *Langmuir* 8 (1992) 3183.
- [20] G.V. Franks, *J. Colloid. Interf. Sci.* 249 (2002) 44.